# Pressure Fluctuations Beneath Instability Wave Packets and Turbulent Spots in a Hypersonic Boundary Layer

SAND2012-2771P

**Katya M. Casper and Steven P. Schneider**
Purdue University

**Steven J. Beresh**
Sandia National Labs

The Johns Hopkins University Applied Physics Laboratory
April 9, 2012

Sandia National Laboratories is a multi-program laboratory managed and operated by Sandia Corporation, a wholly owned subsidiary of Lockheed Martin Corporation, for the U.S. Department of Energy's National Nuclear Security Administration under contract DE-AC04-94AL85000.

# Motivation

- **Pressure fluctuations peak during boundary-layer transition.**
  - Need to model fluctuations and spatial distribution for structural design of reentry vehicles.
  - Also important for vibration of internal components.
- **Seek to develop more accurate model using turbulent-spot approach.**
  - Current models based on incompressible flow data or from noisy tunnels.

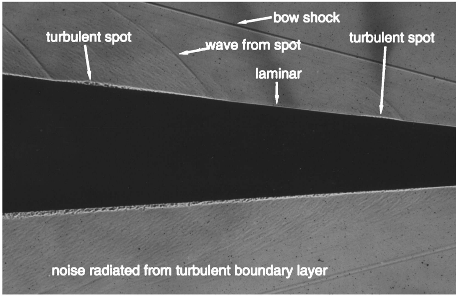


Schlieren image of turbulent spots on a 5° sharp cone at Mach 4.3 in NOL Ballistics Range, from Reda.

# Turbulent Spot Approach to Modeling Transitional Pressure Fluctuations

- Model already developed for pressure fluctuations on a flat plate in incompressible flow.
- Need accurate measurements of the growth and the internal structure of the spots as input to model.
- No previous measurements of internal pressure structure of spots in hypersonic flow.

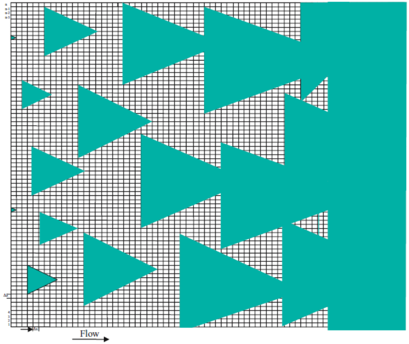


Turbulent spot model simulation, from Vinod (2007).

# Turbulent Spot Geometry

- **Spot growth is characterized by:**
  - Lateral spreading half angle.
  - Front half angle or leading and trailing edge velocities.
- **Spot model also relies on:**
  - Spatial distribution of pressure fluctuations.
  - How spots merge.

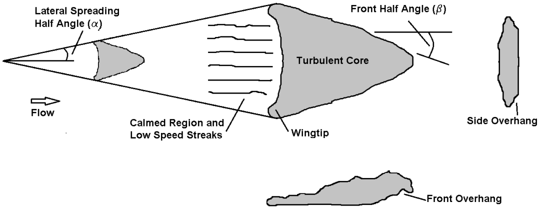


Schematic of a turbulent spot.

# Instability Wave Packets

- **The second-mode instability is one of the dominant boundary-layer instabilities at hypersonic speeds.**
- **Acts like an acoustic wave trapped in the boundary layer.**
  - Reflects between model surface and sonic line in the boundary layer as it travels downstream.
  - Dominant instability is 2D.
- **Appears as rope waves in schlieren images.**

# Boeing/AFOSR Mach-6 Quiet Tunnel (BAM6QT)

- **Ludwieg tube design.**
- **Can be operated under noisy or quiet flow.**
- **For quiet flow:**
  - Contraction boundary layer removed using bleed slots.
  - Laminar boundary layer restarted at throat.
  - Long, highly-polished nozzle to reduce growth of instabilities.
  - Laminar flow is maintained downstream of nozzle exit.

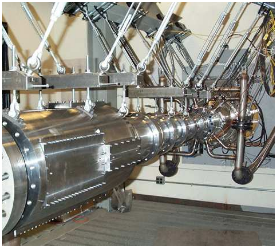

BAM6QT nozzle and test section.

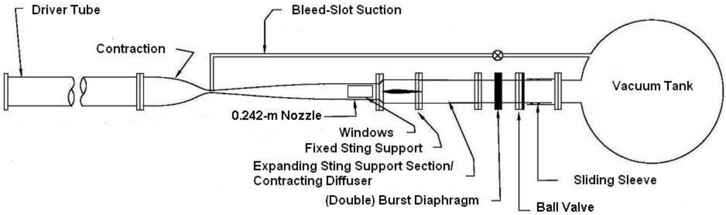

# Conventional vs. Quiet Tunnels

- **Conventional Tunnels**
  - High noise near 2–5% of the mean.
  - Noise can cause much earlier transition than in flight.
- **Quiet Tunnel**
  - Low noise around 0.05%.
  - Comparable to flight.

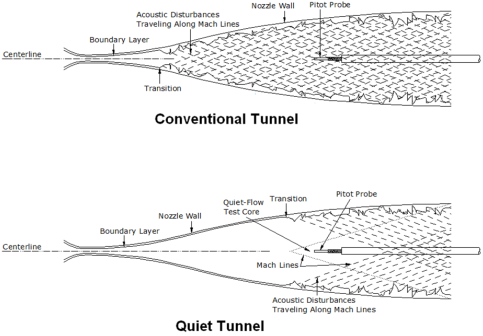


Schematic of difference between conventional and quiet tunnel, from Segura (2007).

# Boeing/AFOSR Mach-6 Quiet Tunnel (BAM6QT)

- **Ludwieg tube design.**
- **Can be operated under noisy or quiet flow.**
- **For quiet flow:**
  - Contraction boundary layer removed using bleed slots.
  - Laminar boundary layer restarted at throat.
  - Long, highly-polished nozzle to reduce growth of instabilities.
  - Laminar flow is maintained downstream of nozzle exit.

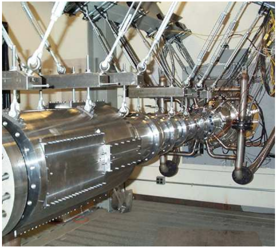

BAM6QT nozzle and test section.

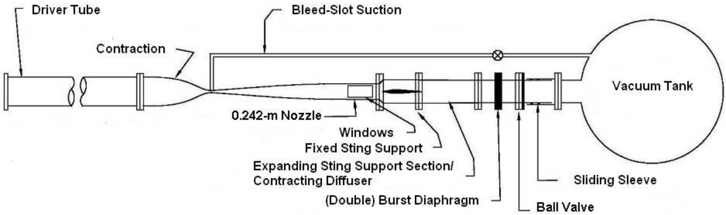

# Previous Pressure Measurements on a 7° Sharp Cone

- **Pressure measurements did not clearly show spots even though statistical evidence pointed to their presence.**
  - Tunnel noise interferes with pressure fluctuation measurements.
    - Transition only occurs on model under noisy flow.
    - Tunnel noise is measured under laminar boundary layer.
  - Frequency response and spatial resolution limitations.
    - Thin boundary layer.

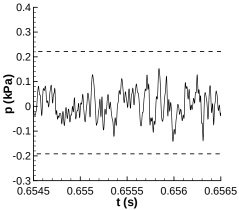


Laminar boundary layer

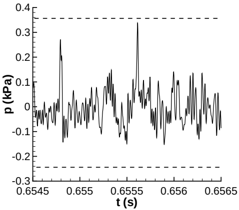


Transitional boundary layer

- **Wall measurements in a quiet tunnel avoid these problems.**
  - Thick, laminar boundary layer.

# Experimental Setup

- **Perturber on top wall of tunnel, upstream of sensors.**
- **Row of Kulite pressure transducers on top wall of tunnel.**
  - 4 sensors in nozzle traverse plug.
  - 5 sensors downstream of nozzle exit in pipe insert.
- **Two spanwise rows of Kulite pressure transducers, one near perturber and one in pipe insert.**

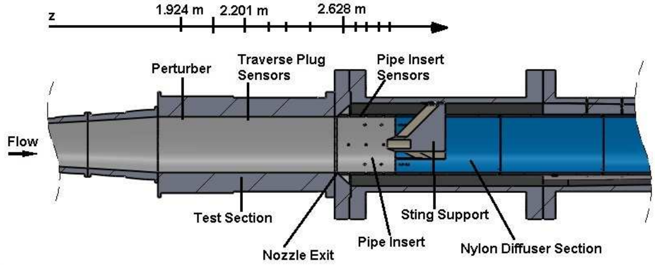


Setup schematic.

# Experimental Setup

- **Pipe insert made of five rings.**
  - Can place spanwise sensor array at four downstream locations.
  - Five sensor locations on either side of tunnel centerline.
- **Location of ring changed during testing.**

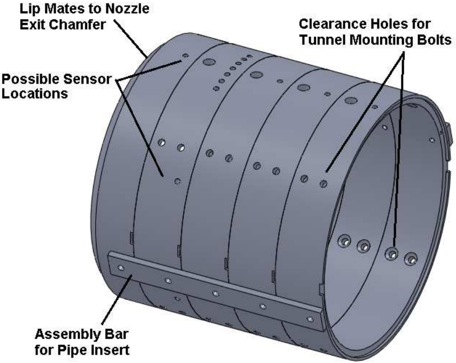


CAD model.

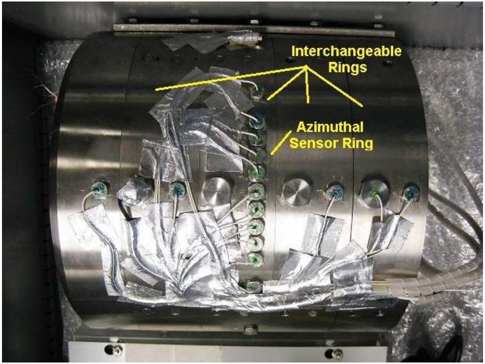


Multi-ring pipe insert.

# Experimental Setup

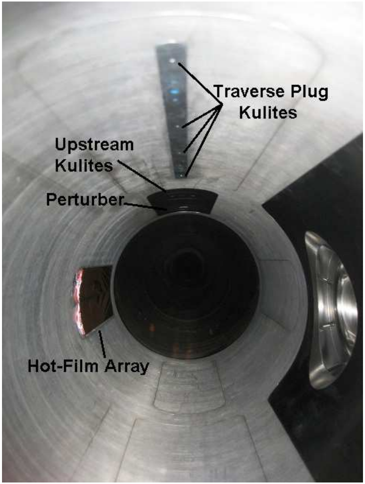


Looking upstream into nozzle.

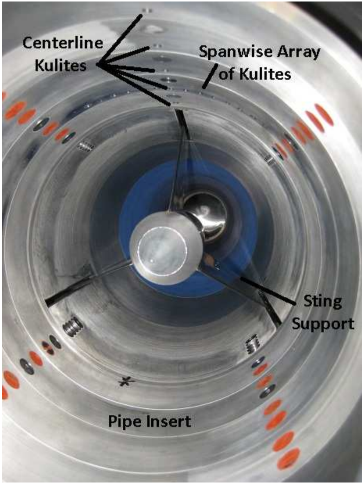


Looking downstream into pipe insert.

# Flow Perturber

- **Two electrodes with gap perpendicular to flow.**
- **Ignition coil and timing circuit used to create perturbations.**
- **Perturbations created at 200 Hz.**
  - Avoids picking up electro-magnetic interference during measurements.
- **50 disturbances are used to compute ensemble-averaged time traces and an averaged power spectral density.**

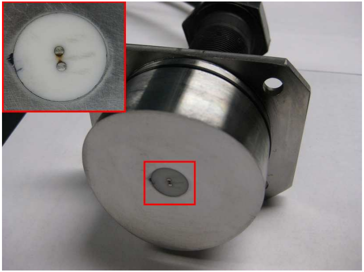

Perturber electrodes.

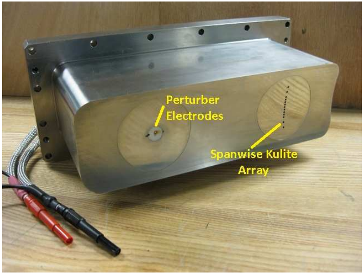


Perturber nozzle-wall insert.

# Instrumentation: Kulite Pressure Transducers (XCQ-062-15A)

- Resonant frequency near 300 kHz.
- A-screen used for frequency measurements up to ∼90 kHz.
- Higher frequency measurements will have some attenuation.

Kulite installed in insert.

# Instrumentation: PCB132 Pressure Transducers

- Piezoelectric-type sensor.
- Resonant frequency above 1 MHz.
- Signal high-pass filtered at 11 kHz.
- Limited spatial resolution.
- Designed as time-of-arrival sensors.
- Have not yet been sufficiently dynamically calibrated.

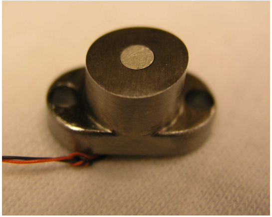

PCB132 installed in insert.

# Instrumentation: ALTP sensors

- High-frequency heat-transfer gage.
- Typical electronics provide AC signal between 17 Hz and 1 MHz and separate DC signal.

ALTP installed in insert.

# Controlled Generation of Nozzle-Wall Disturbances

# Electrical Perturbation Measurements

- **Made voltage and current measurements of perturbation.**
- **Observe a lower-frequency pulse instead of a rapid spark.**
  - Corresponds to a pulsed glow perturbation.
- **Computed PSD of perturbation power.**
  - Dominant frequencies below 30 kHz.
  - Still significant frequency content above 150 kHz.

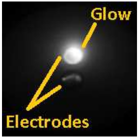


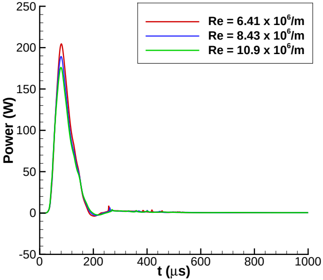


Ensemble-averaged time traces.

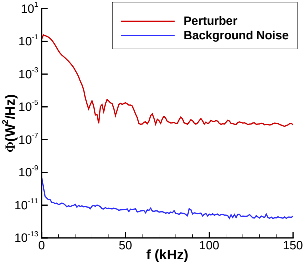


Power spectral density at $Re = 6.41 \times 10^6$/m.

# Electrical Perturbation Measurements

- Higher frequency contribution was investigated.
- Individual samples show deviations from mean near 50 $\mu s$ and 250–500 $\mu s$.
- During initiation of glow pulse, high frequencies are generated.

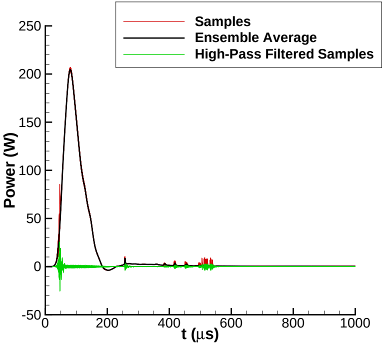


Individual samples and ensemble average.

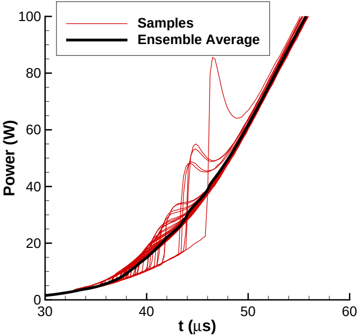


Close-up of high frequencies during glow initiation.

# Centerline Measurements of Controlled Disturbances

# Centerline Measurements at $Re = 6.33 \times 10^6/m$

- Perturbation initially generates a linear wave packet.
- Packet grows and becomes nonlinear by z = 2.679 m.
- Additional peaks appear in the spectra by z = 2.730 m.
- Start to get rise in broadband frequencies by z = 2.831 m.

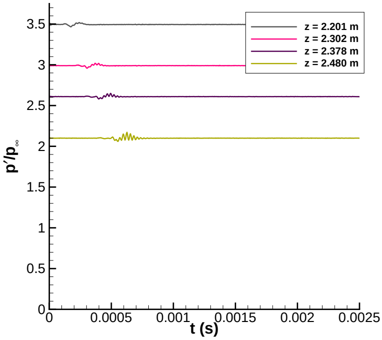


Time traces.

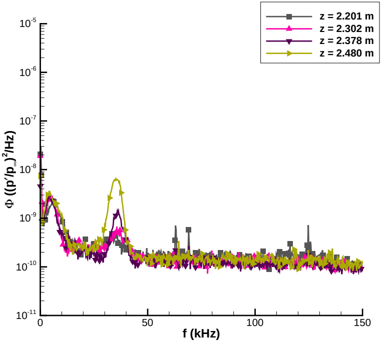


Power spectral density.

# Centerline Measurements at $Re = 6.33 \times 10^6/m$

- Perturbation initially generates a linear wave packet.
- Packet grows and becomes nonlinear by z = 2.679 m.
- Additional peaks appear in the spectra by z = 2.730 m.
- Start to get rise in broadband frequencies by z = 2.831 m.

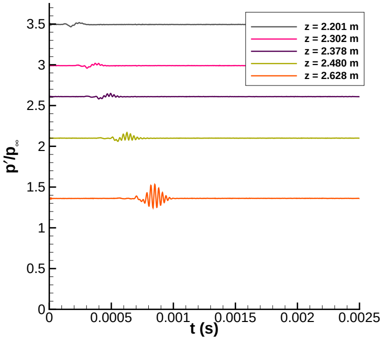


Time traces.

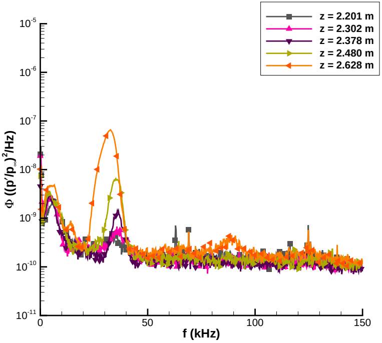


Power spectral density.

# Centerline Measurements at $Re = 6.33 \times 10^6/m$

- Perturbation initially generates a linear wave packet.
- Packet grows and becomes nonlinear by z = 2.679 m.
- Additional peaks appear in the spectra by z = 2.730 m.
- Start to get rise in broadband frequencies by z = 2.831 m.

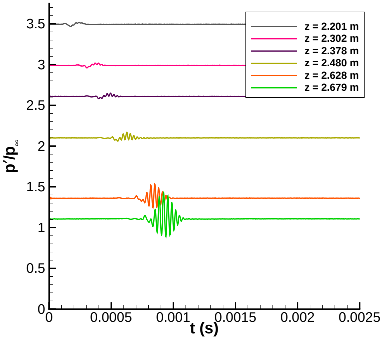


Time traces.

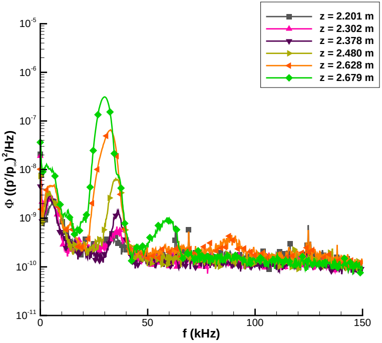


Power spectral density.

# Centerline Measurements at $Re = 6.33 \times 10^6/m$

- Perturbation initially generates a linear wave packet.
- Packet grows and becomes nonlinear by z = 2.679 m.
- Additional peaks appear in the spectra by z = 2.730 m.
- Start to get rise in broadband frequencies by z = 2.831 m.

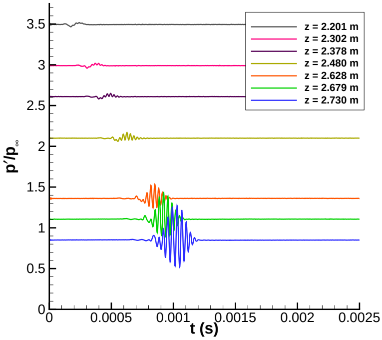


Time traces.

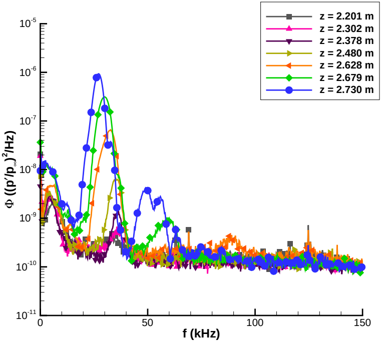


Power spectral density.

# Centerline Measurements at $Re = 6.33 \times 10^6/m$

- Perturbation initially generates a linear wave packet.
- Packet grows and becomes nonlinear by z = 2.679 m.
- Additional peaks appear in the spectra by z = 2.730 m.
- Start to get rise in broadband frequencies by z = 2.831 m.

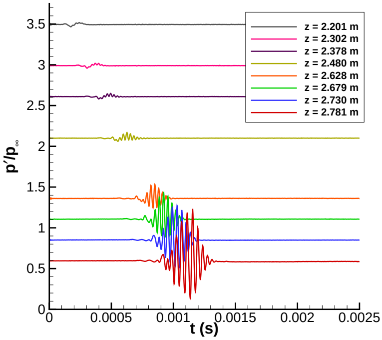


Time traces.

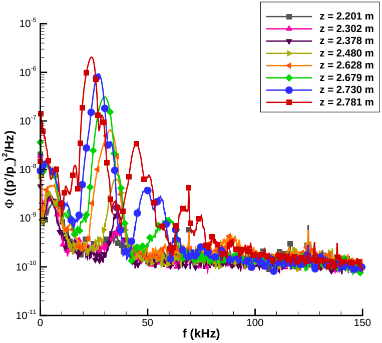


Power spectral density.

# Centerline Measurements at $Re = 6.33 \times 10^6/m$

- Perturbation initially generates a linear wave packet.
- Packet grows and becomes nonlinear by z = 2.679 m.
- Additional peaks appear in the spectra by z = 2.730 m.
- Start to get rise in broadband frequencies by z = 2.831 m.

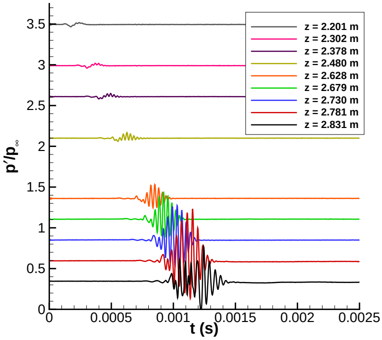


Time traces.

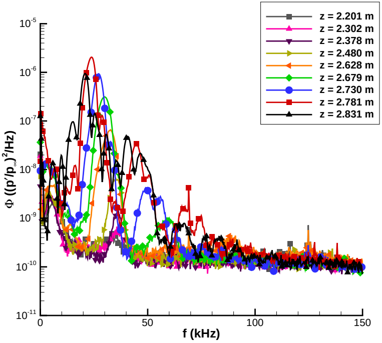


Power spectral density.

# Centerline Measurements at $Re = 8.25 \times 10^6$/m

- Small second-mode waves grow and develop along nozzle length.
- Peak frequency is $\sim$30–40 kHz.
- Large amplitude fluctuations visible before breakdown.
- Second-mode waves still visible on either side of turbulent fluctuations.

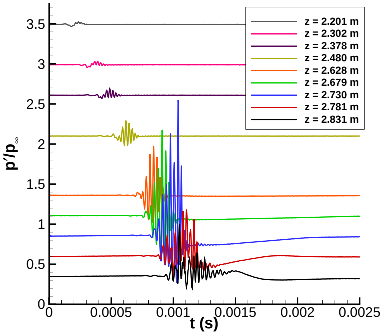


Time traces.

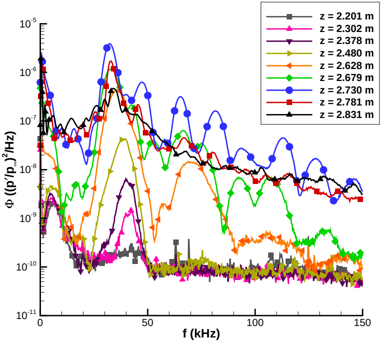


Power spectral density.

# Centerline Measurements at $Re = 10.8 \times 10^6/m$

- Second-mode waves grow larger in amplitude further upstream.
- Peak frequency is ∼45–50 kHz.
- Breakdown occurs before pipe insert sensors.
- Second-mode waves still visible on either side of turbulent fluctuations.

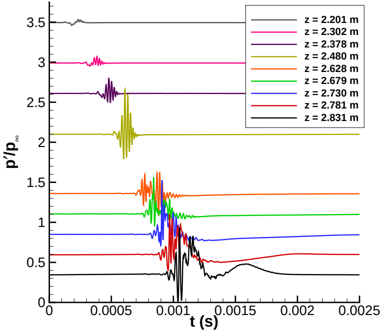


Time traces.

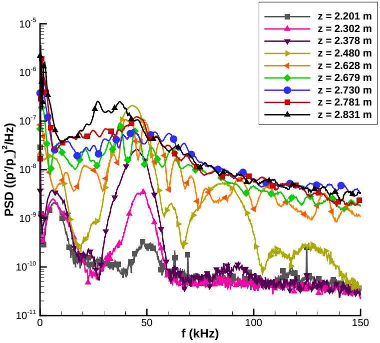


Power spectral density.

# Deviation of Individual Samples from Ensemble Average at $Re = 8.25 \times 10^6/m$

- Samples show good repeatability through breakdown.
- Average traces do not represent samples once they breakdown.
- Power spectral density computed from traces shows average frequency content of disturbances.

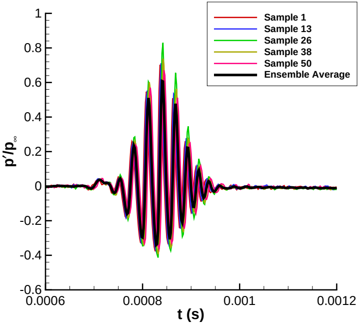


z = 2.628 m

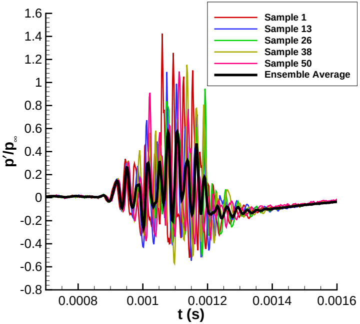


z = 2.831 m

# Comparison of Kulite and ALTP Ensemble Averages at $Re = 5.76 \times 10^6/m$

- Can verify results by comparing to other sensors.
- Kulite data compared to nearby heat-transfer ALTP gages.
- Sensors show similar wave packet structures, but differences arise at higher *Re*.

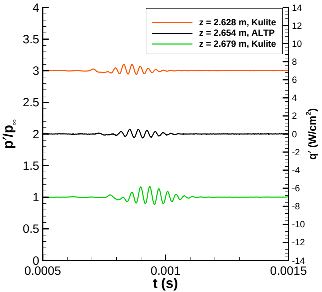


Time traces.

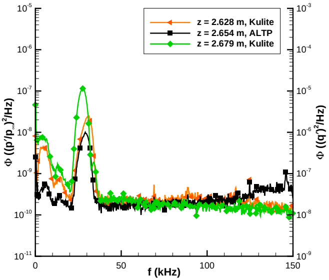


Power spectral density.

# Comparison of Kulite and ALTP Ensemble Averages at $Re = 8.25 \times 10^6/m$

- Can verify results by comparing to other sensors.
- Kulite data compared to nearby heat-transfer ALTP gages.
- Sensors show similar wave packet structures, but differences arise at higher *Re*.

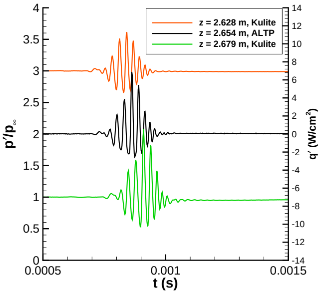


Time traces.

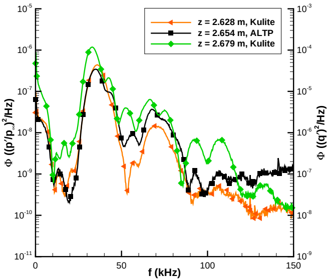


Power spectral density.

# Comparison of Kulite and ALTP Ensemble Averages at $Re = 10.8 \times 10^6/m$

- Can verify results by comparing to other sensors.
- Kulite data compared to nearby heat-transfer ALTP gages.
- Sensors show similar wave packet structures, but differences arise at higher *Re*.

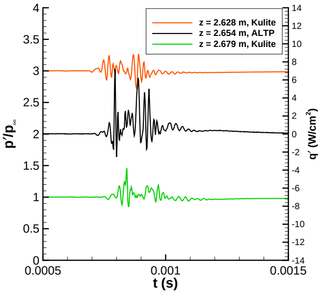


Time traces.

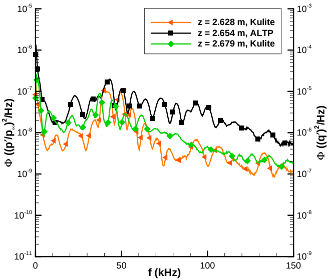


Power spectral density.

# Verification with Other Sensors, $Re = 5.80 \times 10^6/m$

- Can also compare to other pressure sensors (PCB132 and PCB113).
- All sensors show wave packets, but there are differing electronic noise levels.
- ALTP has best signal-to-noise ratio, PCB113 has the worst.

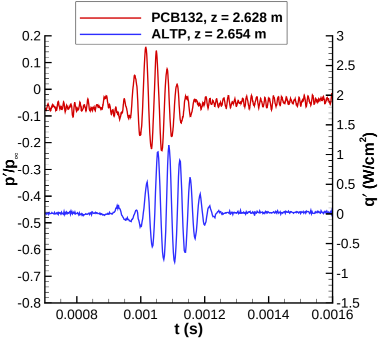


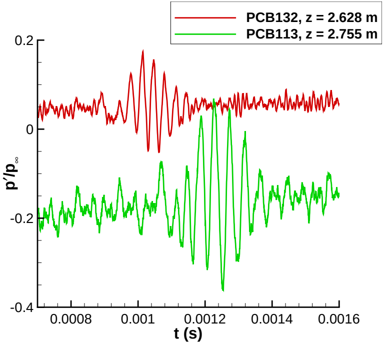

# Spanwise Distribution of Pressure Fluctuations within Controlled Disturbances

# Spanwise Measurements at $Re = 6.33 \times 10^6/m$, z = 2.679 m

- Spanwise Kulite array used to observe off-center disturbance structure.
- Largest waves occur near the centerline.
- Some asymmetry in these measurements.

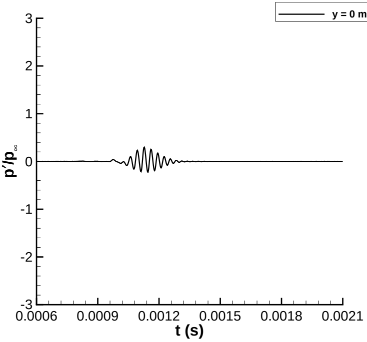


Time traces.

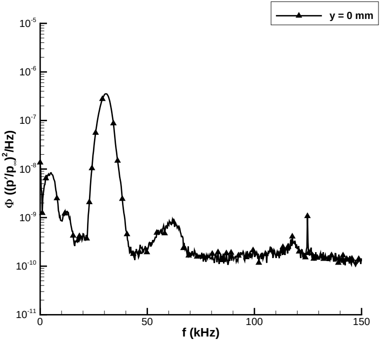


Power spectral density.

# Spanwise Measurements at $Re = 6.33 \times 10^6/m$, z = 2.679 m

- Spanwise Kulite array used to observe off-center disturbance structure.
- Largest waves occur near the centerline.
- Some asymmetry in these measurements.

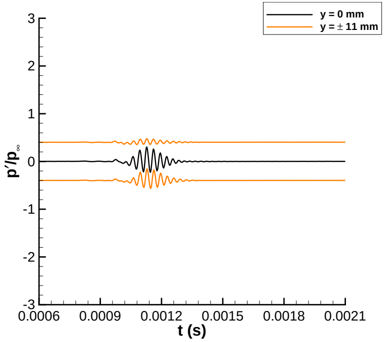


Time traces.

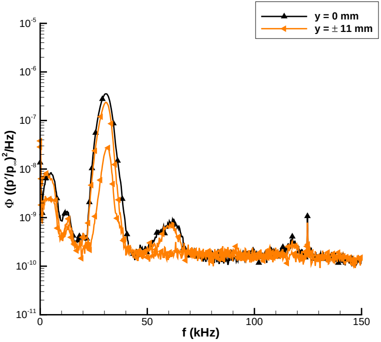


Power spectral density.

# Spanwise Measurements at $Re = 6.33 \times 10^6/m$, z = 2.679 m

- Spanwise Kulite array used to observe off-center disturbance structure.
- Largest waves occur near the centerline.
- Some asymmetry in these measurements.

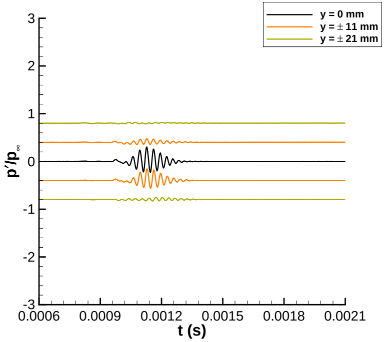


Time traces.

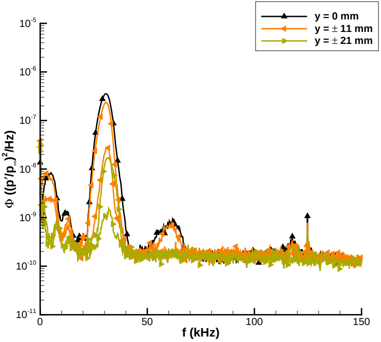


Power spectral density.

# Spanwise Measurements at $Re = 6.33 \times 10^6/m$, z = 2.679 m

- Spanwise Kulite array used to observe off-center disturbance structure.
- Largest waves occur near the centerline.
- Some asymmetry in these measurements.

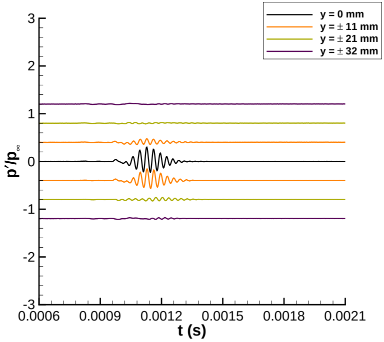


Time traces.

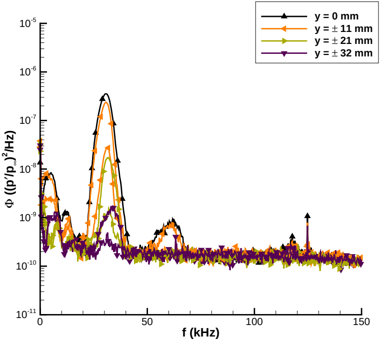


Power spectral density.

# Spanwise Measurements at $Re = 6.33 \times 10^6/m$, z = 2.679 m

- Spanwise Kulite array used to observe off-center disturbance structure.
- Largest waves occur near the centerline.
- Some asymmetry in these measurements.

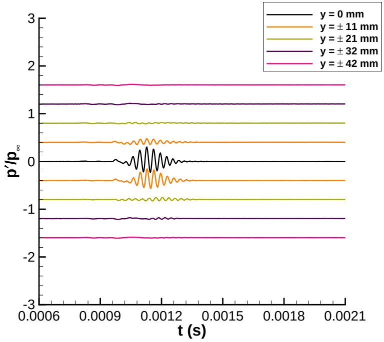


Time traces.

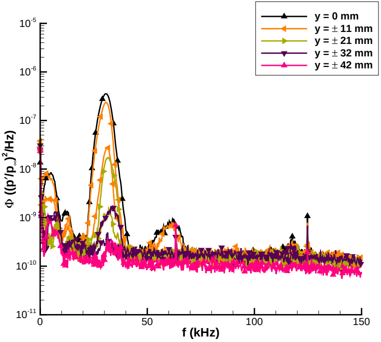


Power spectral density.

# Spanwise Measurements at $Re = 6.33 \times 10^6/m$, z = 2.679 m

- Spanwise Kulite array used to observe off-center disturbance structure.
- Largest waves occur near the centerline.
- Some asymmetry in these measurements.

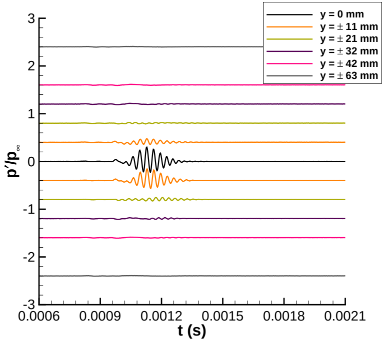


Time traces.

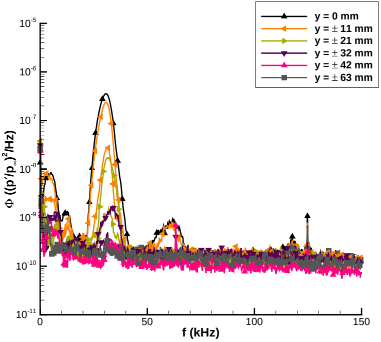


Power spectral density.

# Spanwise Measurements at $Re = 6.33 \times 10^6/m$, z = 2.730 m

- Wave amplitudes grow further downstream.
- By z = 2.831 m, averaged wave amplitude decreases.
- Some waves may be breaking down, leading to smaller averaged amplitudes and more broadband frequencies in the PSD.

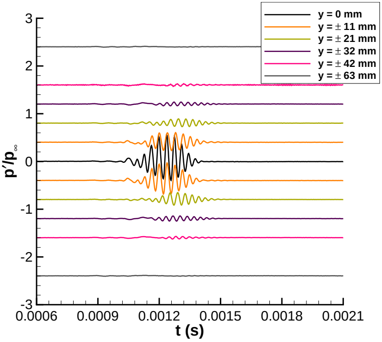


Time traces.

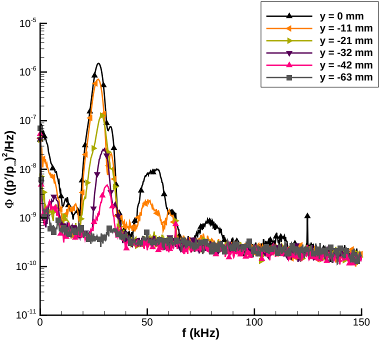


Power spectral density.

# Spanwise Measurements at $Re = 6.33 \times 10^6/m$, z = 2.781 m

- Wave amplitudes grow further downstream.
- By z = 2.831 m, averaged wave amplitude decreases.
- Some waves may be breaking down, leading to smaller averaged amplitudes and more broadband frequencies in the PSD.

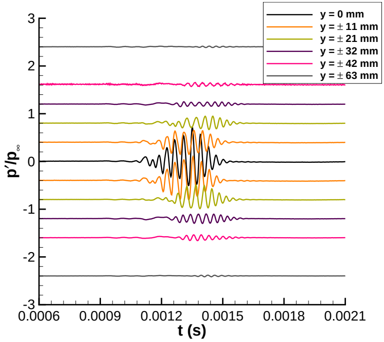


Time traces.

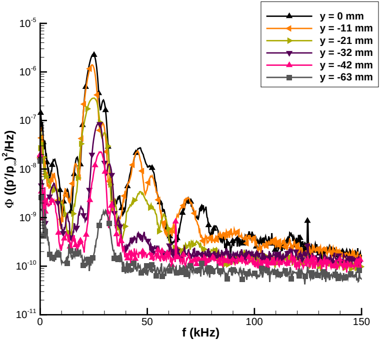


Power spectral density.

# Spanwise Measurements at $Re = 6.33 \times 10^6/m$, z = 2.831 m

- Wave amplitudes grow further downstream.
- By z = 2.831 m, averaged wave amplitude decreases.
- Some waves may be breaking down, leading to smaller averaged amplitudes and more broadband frequencies in the PSD.

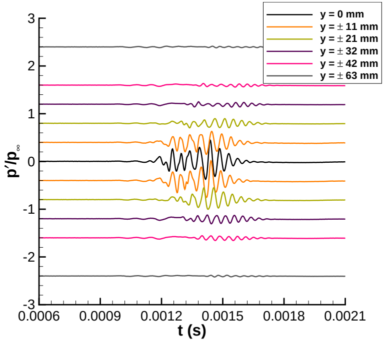


Time traces.

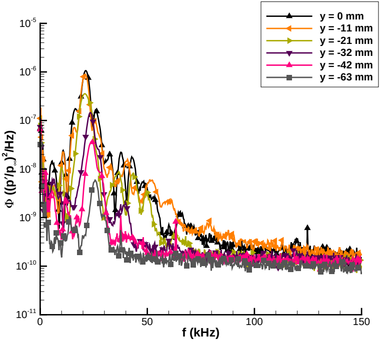


Power spectral density.

# Contour Plots of Spanwise Measurements at $Re = 6.3 \times 10^6/m$

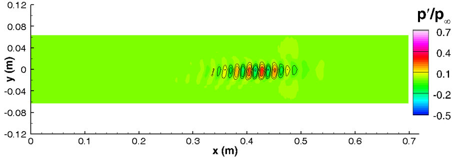


(a) z = 2.679 m

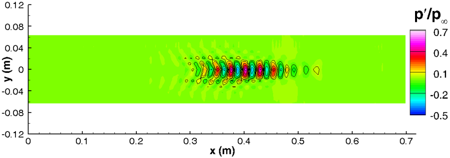


(b) z = 2.730 m

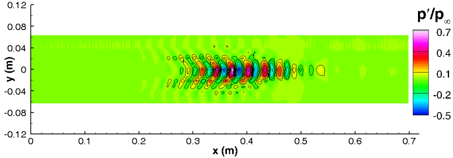


(c) z = 2.781 m

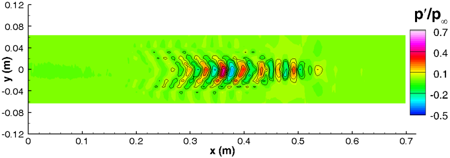


(d) z = 2.831 m

# Contour Plots of Spanwise Measurements at $Re = 6.3 \times 10^6/m$

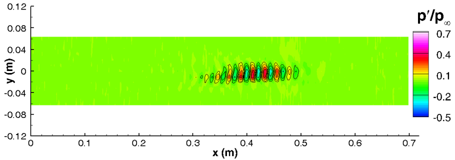


(e) z = 2.679 m

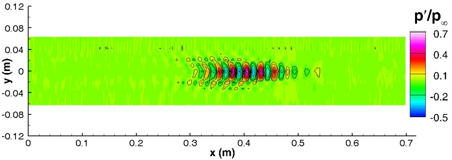


(f) z = 2.730 m

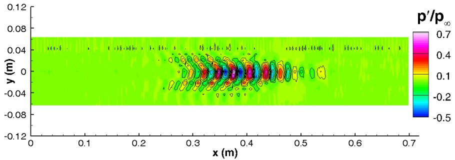


(g) z = 2.781 m

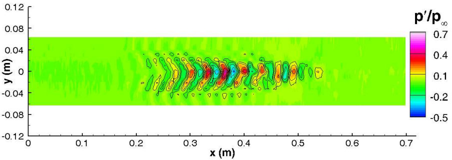


(h) z = 2.831 m

# Spanwise Measurements at $Re = 8.3 \times 10^6/m$, z = 2.679 m

- Spanwise measurements agree with centerline results.
- Large second-mode waves near centerline.
- Waves decrease in amplitude further from centerline.
- Breakdown of the waves begins in the center of the disturbances.

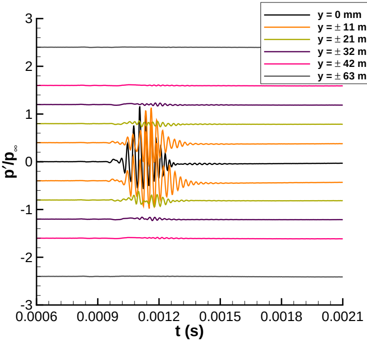


Time traces.

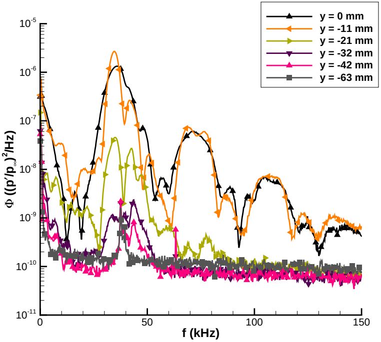


Power spectral density.

# Spanwise Measurements at $Re = 8.3 \times 10^6/m$, z = 2.730 m

- Spanwise measurements agree with centerline results.
- Large second-mode waves near centerline.
- Waves decrease in amplitude further from centerline.
- Breakdown of the waves begins in the center of the disturbances.

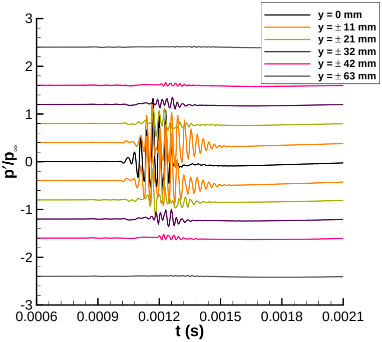


Time traces.

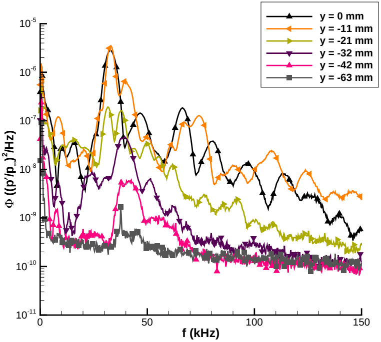


Power spectral density.

# Spanwise Measurements at $Re = 8.3 \times 10^6/m$, z = 2.781 m

- Further downstream, waves break down on centerline.
- Broadband frequencies observed in spectra.
- Second-mode waves still observed at front, rear, and spanwise edges of spots.

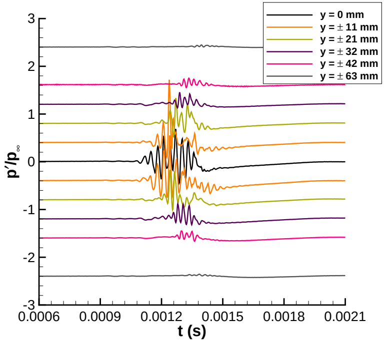


Time traces.

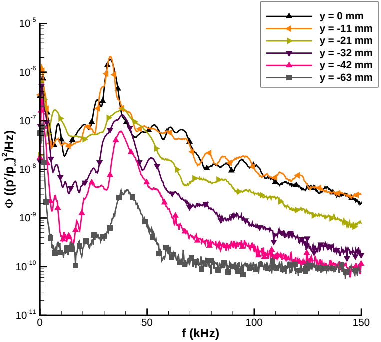


Power spectral density.

# Spanwise Measurements at $Re = 8.3 \times 10^6/m$, z = 2.831 m

- Further downstream, waves break down on centerline.
- Broadband frequencies observed in spectra.
- Second-mode waves still observed at front, rear, and spanwise edges of spots.

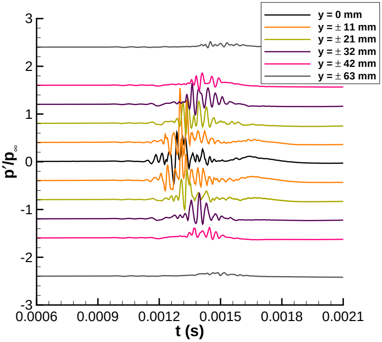


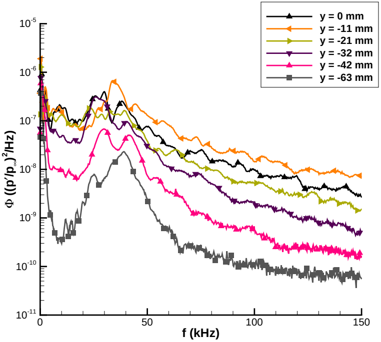


Time traces.

Power spectral density.

# Contour Plots of Spanwise Measurements near $Re = 8.30 \times 10^6/m$

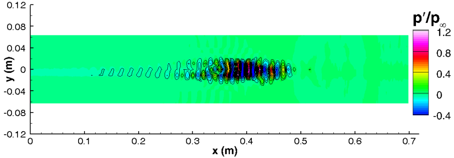


(a) z = 2.679 m

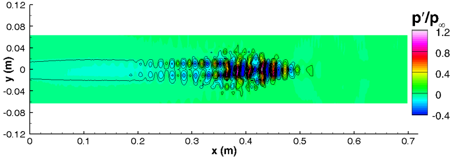


(b) z = 2.730 m

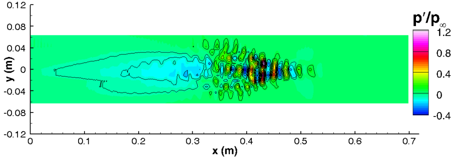


(c) z = 2.781 m

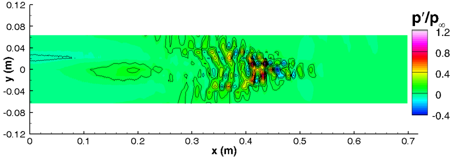


(d) z = 2.831 m

# Contour Plots of Spanwise Measurements near $Re = 8.30 \times 10^6/m$

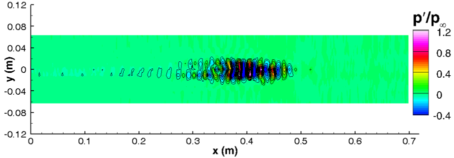


(e) z = 2.679 m

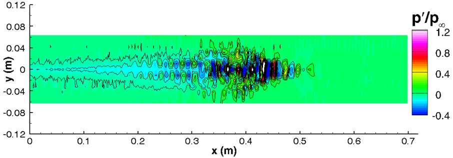


(f) z = 2.730 m

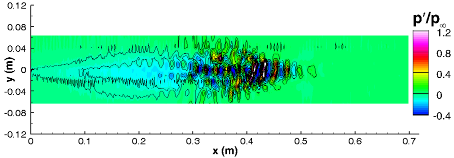


(g) z = 2.781 m

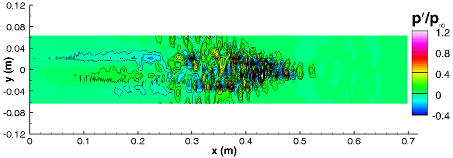


(h) z = 2.831 m

# Spanwise Measurements at $Re = 10.8 \times 10^6/m$, z = 2.679 m

- Characteristic arrowhead shape of turbulent spots is seen.
- Turbulent fluctuations are observed near center.
- Second-mode waves persist at spanwise edges.
- Waves also observed in front and rear of spots.

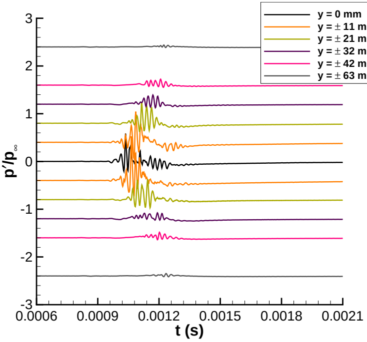


Time traces.

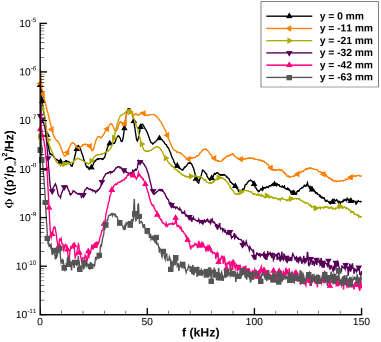


Power spectral density.

# Spanwise Measurements at $Re = 10.8 \times 10^6/m$, z = 2.730 m

- Characteristic arrowhead shape of turbulent spots is seen.
- Turbulent fluctuations are observed near center.
- Second-mode waves persist at spanwise edges.
- Waves also observed in front and rear of spots.

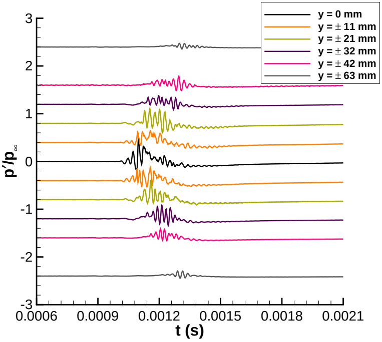


Time traces.

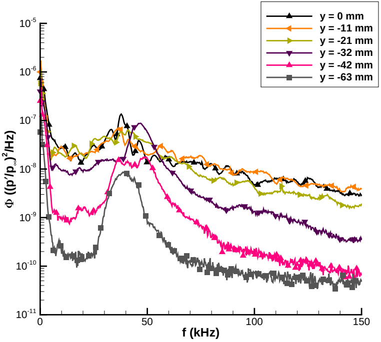


Power spectral density.

# Spanwise Measurements at $Re = 10.8 \times 10^6/m$, z = 2.781 m

- Characteristic arrowhead shape of turbulent spots is seen.
- Turbulent fluctuations are observed near center.
- Second-mode waves persist at spanwise edges.
- Waves also observed in front and rear of spots.

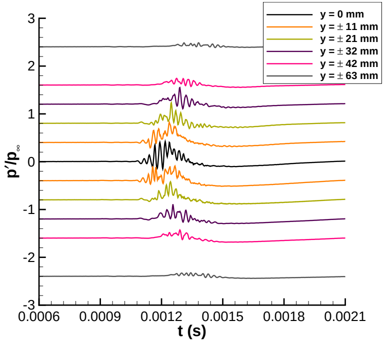


Time traces.

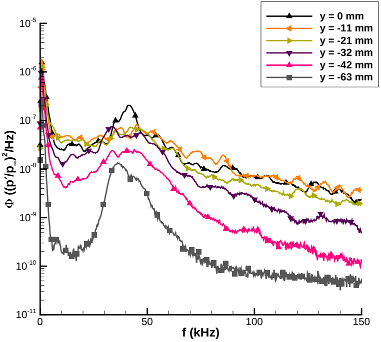


Power spectral density.

# Spanwise Measurements at $Re = 10.8 \times 10^6/m$, z = 2.831 m

- Characteristic arrowhead shape of turbulent spots is seen.
- Turbulent fluctuations are observed near center.
- Second-mode waves persist at spanwise edges.
- Waves also observed in front and rear of spots.

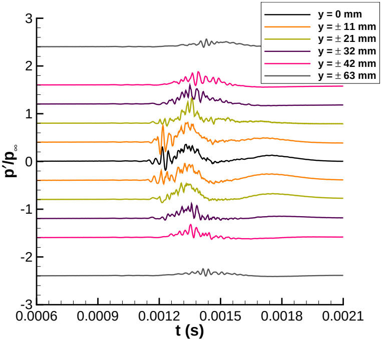


Time traces.

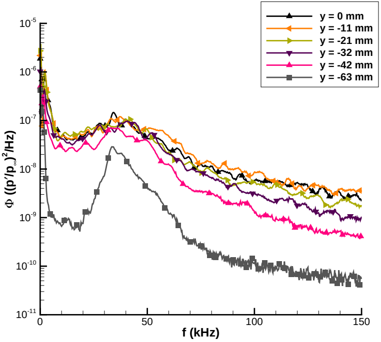


Power spectral density.

# Contour Plots of Spanwise Measurements at $Re = 10.8 \times 10^6/m$

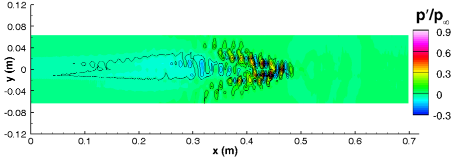


(a) z = 2.679 m

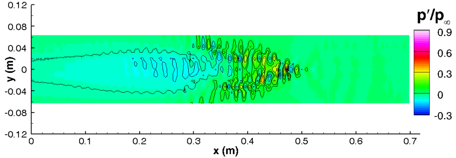


(b) z = 2.730 m

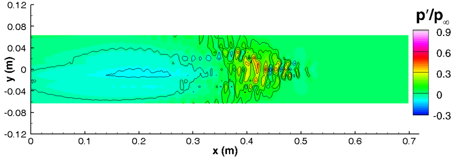


(c) z = 2.781 m

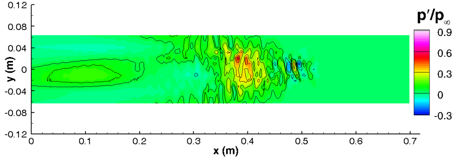


(d) z = 2.831 m

# Contour Plots of Spanwise Measurements at $Re = 10.8 \times 10^6/m$

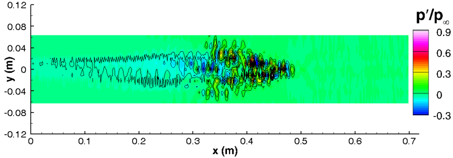


(e) z = 2.679 m

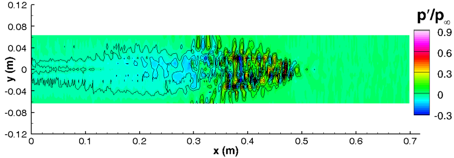


(f) z = 2.730 m

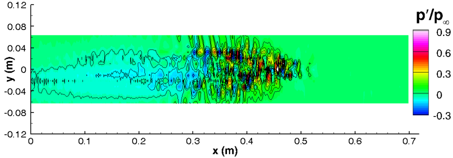


(g) z = 2.781 m

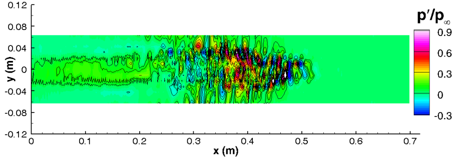


(h) z = 2.831 m

# Natural Growth of Nozzle-Wall Disturbances

# Large Turbulent Spot at $Re = 11.2 \times 10^6/m$

- Spots originate near throat and grow large along nozzle length.
- Cover majority of nozzle circumference.
- Occur more frequently at higher *Re*.
- Last sensor shows a second pressure peak behind the spot.

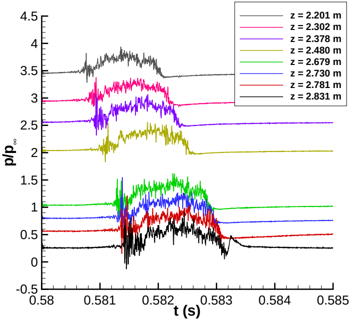


Time traces.

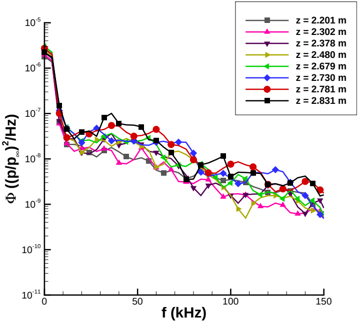


Power spectral density.

# Natural Nozzle Wall Disturbances: Second-Mode Disturbances at $Re = 10.6 \times 10^6/m$

- Small disturbances originate further downstream on nozzle wall.
- Wave packets agree with computed second-mode frequencies.
- Packets breakdown into turbulent spots.
- Occur more frequently at higher *Re*.

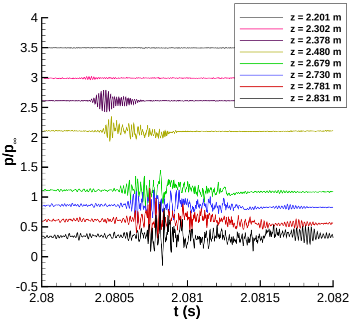


Time traces.

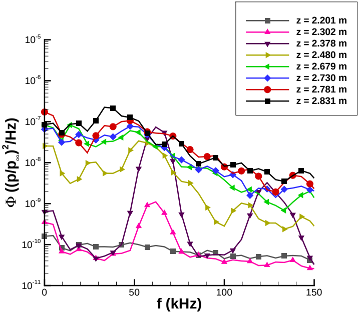


Power spectral density.

# Spanwise Distribution of Pressure Fluctuations, $Re$ near $10.8 \times 10^6/m$

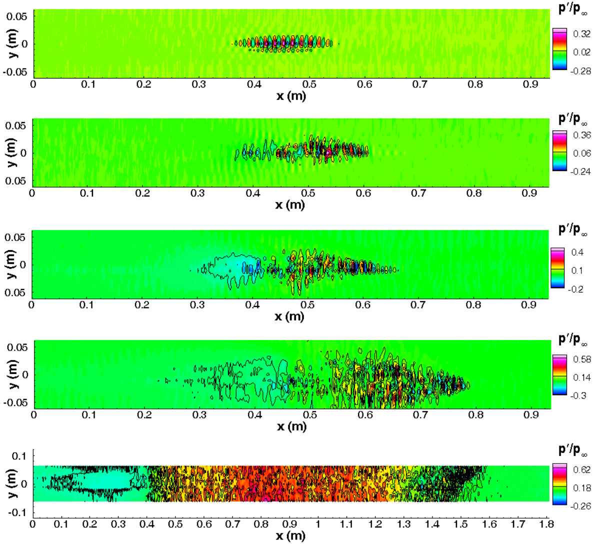

# Turbulent-Spot Model Parameters

# Convection Velocities Near $Re = 11.0 \times 10^6/m$

- Average leading edge convection velocity of 0.95 $U_\infty$.
- Trailing edge convection velocity varies with *Re* between 0.64–0.75 $U_\infty$.
- Computed velocities agree well with natural disturbances, DNS, and other experiments.

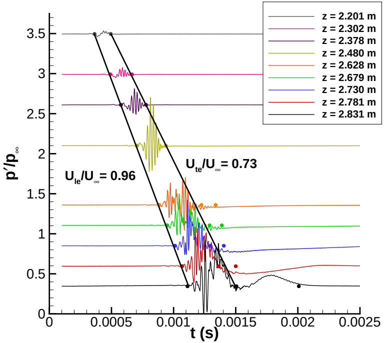


Controlled disturbances.

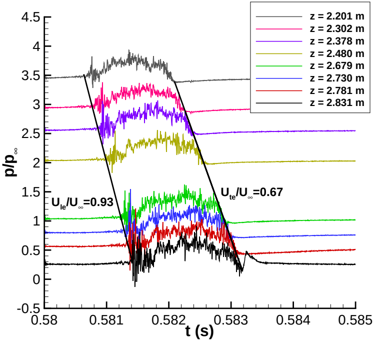


Naturally developing turbulent spots.

# Lateral Spreading Angle of Disturbances, $Re = 8.30 \times 10^6/m$

- **Triangular footprint was estimated for disturbances at four downstream locations.**
  - Lateral edges of disturbances as they change downstream are used to compute lateral spreading angle.
- **Found angle of $\sim$15 degrees, much higher than expected.**
  - High-frequency pressure fluctuations have never been used to define the spot footprint before.
  - May provide a different spreading angle than other experimental or computational methods.

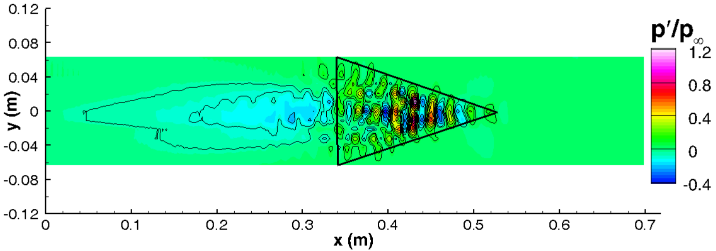

# Low-Frequency Component of Disturbances

- Time traces near $Re = 10.8 \times 10^6/m$ were low-pass filtered at 15 kHz to look at mean pressure change within disturbances.
- Higher mean pressure in core, $\sim$20–30% above $p_\infty$.
- Low pressure calmed region behind spots, $\sim$10% below $p_\infty$.

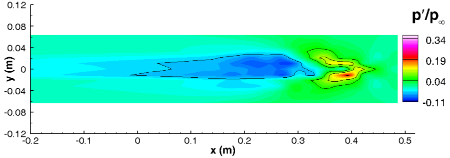


(a) z = 2.679 m

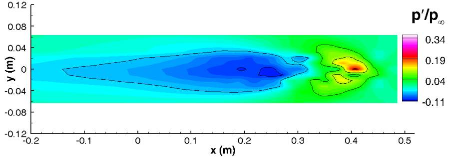


(b) z = 2.730 m

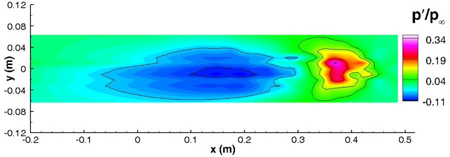


(c) z = 2.781 m

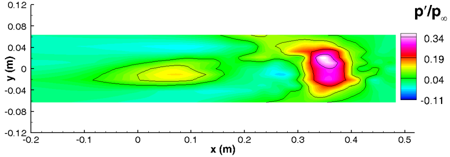


(d) z = 2.831 m

# Turbulent Spot Model Parameters

- **Spot growth is characterized by:**
  - ✓ Lateral spreading half angle.
  - ✓ Leading and trailing edge convection velocities.
- **Spot model also relies on:**
  - ✓ Spatial distribution of pressure fluctuations.
  - ✗ How spots merge.

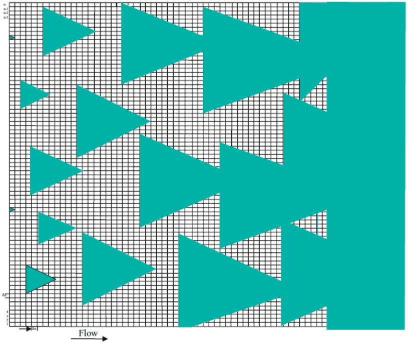


Turbulent spot model simulation, from Vinod (2007).

# Controlled Perturbations on a Seven-Degree Cone

# Controlled Perturbations on a Seven-Degree Cone: Experimental Setup

- Glow perturber was placed on cone.
- Followed by a line of 8 sensors along centerline.
- A mix of Kulite, PCB132, and ALTP sensors were used.
- Results shown here are from a PCB132 midway down cone.

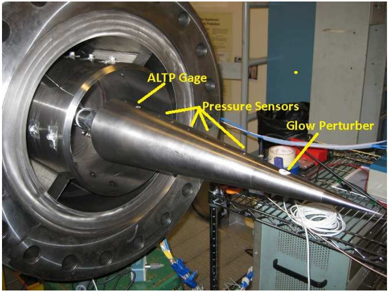


Cone installed in BAM6QT for glow-perturber tests.

# PCB132 Results at varying *Re*

- **Similar perturbations used to generate ensemble averages.**
  - Still scatter from sample to sample.
- **Can see second-mode wave packet at low *Re*.**
- **Becomes turbulent at high *Re*.**
- **Appears similar to transitional physics on nozzle wall.**

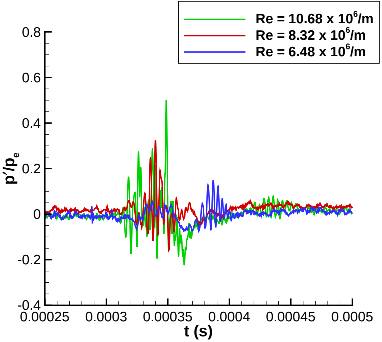


Time traces of individual samples.

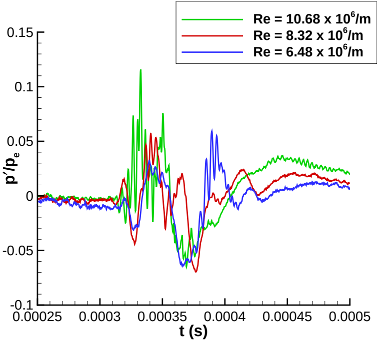


Ensemble-averaged time traces.

# PCB132 Results at varying *Re*

- **Similar perturbations used to generate ensemble averages.**
  - Still scatter from sample to sample.
- **Can see second-mode wave packet at low *Re*.**
- **Becomes turbulent at high *Re*.**
- **Appears similar to transitional physics on nozzle wall.**

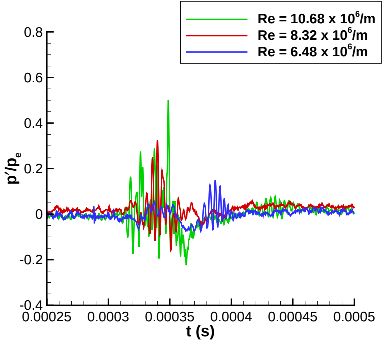


Time traces of individual samples.

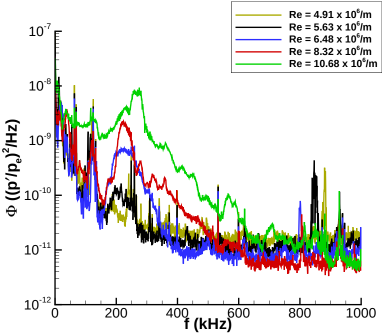


Power spectral density.

# Conclusions

- **Thick nozzle-wall boundary layer allows resolution of boundary-layer disturbances with pressure instrumentation.**
- **Wave packets:**
  - Smaller wave packets are ordered and concentrated near the centerline.
  - Larger wave packets become distorted.
  - Weaker second-mode disturbances extend in spanwise direction.
- **Turbulent spots:**
  - At higher *Re*, wave packets break down to turbulence in center of spots.
  - See characteristic arrowhead shape of turbulent spots.
  - At edges, front, and rear of spots, second-mode waves are still observed and dominate the spectra.

# Conclusions

- **Natural disturbances:**
  - Two disturbances primarily seen at higher *Re*.
    - Large turbulent spots growing from near throat.
    - Second-mode waves breaking down to turbulent spots further downstream in nozzle.
  - Natural disturbances have similar characteristics to controlled disturbances.
- **Development of turbulent-spot model:**
  - Experiments provide convection velocity, spreading angle, and pressure-fluctuation field of disturbances.
  - Still need to address what happens as disturbances merge.
- **Extension to a seven-degree cone:**
  - Wave packets and turbulent spots can be created and studied on cone with available pressure instrumentation.
  - Growth and breakdown of waves appears similar to nozzle wall, but improved measurements needed.

# Suggestions for Future Work

- **Increase measurement length to study more developed spots and spot merging.**
  - Can use a pipe-insert extension to double measurement length.
  - Can better study longitudinal spot merging.
  - Can place two perturbers 90 degrees apart to study lateral spot merging.
- **Improved cone measurements.**
  - Need centerline measurements with a line of PCB132 sensors.
  - Need spanwise measurements.
- **Comparisons to DNS computations.**
- **Iterations with model developers.**